Available online at www.sciencedirect.com
SCIENCE DIRECT®
Catalysis Today 111 (2006) 212–216
CATALYSIS TODAY
www.elsevier.com/locate/cattod

Selective oxidation of hydrogen sulfide containing excess water and ammonia over vanadia–titania aerogel catalysts

M.I. Kim [a], D.W. Park [a,*], S.W. Park [a], X. Yang [a], J.S. Choi [b], D.J. Suh [b]

[a] *Division of Chemical Engineering, Pusan National University, Kumjeong-ku, Busan 609-735, Republic of Korea*
[b] *Clean Technology Research Center, Korea Institute of Science and Technology, Seongbuk-ku, Seoul 136-791, Republic of Korea*

Abstract

A series of V_2O_5–TiO_2 aerogel catalysts were prepared by sol–gel method with subsequent supercritical drying with CO_2. The aerogel catalysts showed much higher surface areas and total pore volumes than V_2O_5–TiO_2 xerogel and impregnated V_2O_5–TiO_2 catalysts. Two species of surface vanadium in the aerogel catalysts were identified by Raman measurements: monomeric vanadyl and polymeric vanadates. The selective oxidation of hydrogen sulfide in the presence of excess water and ammonia was studied over these catalysts. Aerogel catalysts showed very high conversion of H_2S without harmful emission of SO_2. Temperature programmed reduction (TPR), XRD and Raman analyses revealed that the high catalytic performance of the aerogel catalysts originated from their highly dispersed VO_x species and high reducibility.

Keywords: Hydrogen sulfide; Selective oxidation; Vanadia–titania; Aerogel

---

1. Introduction

Since the international environmental regulations concerning the release of sulfur containing gas become more stringent, hydrogen sulfide contained in the acid gases should be effectively recovered before emission to atmosphere. For many years, most of hydrogen sulfide in petroleum refineries and natural gas plants has been removed by the well-known Claus process [1,2]. A mixed gas of H_2S, NH_3 and water vapor is released from steel smelting processes where the H_2S from coke ovens is generally scrubbed and concentrated using aqueous ammonia solution. The concentrated H_2S is separated from the solution and transferred to the Claus plant. However, the separation of H_2S from the solution is not perfect and the remaining aqueous ammonia stream contains about 2% H_2S, which in turn causes the SO_x emission problem during incineration. In this case, the control of SO_x emission is difficult because the stream contains not only excess water vapor but also high concentration of ammonia. One approach to resolve the problem is the selective catalytic oxidation of H_2S to ammonium thiosulfate (ATS) and elemental sulfur as reported in our previous works [3–5]. We reported a new vapor phase catalytic process for the selective conversion of H_2S in a stream containing both ammonia and water. Vanadium-based mixed oxides, VO_x/TiO_2 and Nb–Fe mixed oxides showed good catalytic activities in the selective oxidation of H_2S to ATS and sulfur.

The conventional processes for the production of ATS are based on the liquid phase reactions. The ATS Claus tail gas clean-up process [6] is divided into two sections: absorption of SO_2 from incinerator in aqueous ammonia and conversion of the intermediate product to ATS by sparging H_2S into the converter. In another ATS process [7], sulfuric acid is reacted with aqueous ammonia solution below 45 °C, then the mixture is contacted with H_2S to form ATS. Therefore, our process has an advantage of direct vapor phase operation compared to the above two processes.

Vanadium–titanium oxides constitute a well-known catalytic system for selective oxidation reactions [8,9]. The outstanding catalytic behavior of vanadia supported on titania is attributed to the strong support-active phase interaction. It has been shown that a higher activity and selectivity is achieved when vanadia is supported on anatase rather than on rutile. The major disadvantage of the titania support prepared by conventional ceramic processes is its low specific surface area.

---

* Corresponding author. Tel.: +82 51 510 2399; fax: +82 51 512 8563.
E-mail address: dwpark@pusan.ac.kr (D.W. Park).

0920-5861/$ – see front matter © 2005 Elsevier B.V. All rights reserved.
doi:10.1016/j.cattod.2005.10.028

The sol–gel method has been proposed as an alternative to synthesize catalysts with a high surface area and stable active phase [10–13]. Several procedures have been proposed: co-gelling of vanadia and titania [11,12], preparation of aerogels by two-step procedure [14], impregnation of V_2O_5 on TiO_2 aerogels [15,16] and hydrogels [17]. In all these studies, V_2O_5 was either immobilized on pre-formed anatase or vanadium and titanium oxides were allowed to gel by a procedure that favors the anatase formation.

The present work focuses on the preparation of V_2O_5–TiO_2 aerogel catalysts using sol–gel method with subsequent drying at supercritical condition. The catalytic performance of the aerogel catalysts was studied for the selective oxidation of H_2S in the stream containing both ammonia and water. V_2O_5–TiO_2 xerogel and V_2O_5–TiO_2 impregnated vanadia–titania catalysts were also prepared to compare their catalytic activities with the aerogel catalysts.

2. Experimental

2.1. Catalyst preparation

V_2O_5–TiO_2 aerogel catalysts with different contents of V_2O_5 were synthesized by using a sol–gel method reported previously [13]. All reagents were used without further purification. A homogeneous solution was prepared by dissolving desired amounts of titanium butoxide (Aldrich) and vanadium oxytriisopropoxide (Aldrich) in a mixture of ethanol (Merck) and nitric acid (Merck) with molar ratio of $EtOH:Ti:HNO_3 = 30:1:0.1$. Then water is slowly added to form a gel. The gel was vigorously stirred for 5 min and maintained at rest at room temperature. After 3 days of aging the resulting gel was dried at supercritical condition with CO_2 at 60 °C and 200 atm. The calcination was carried out in air at a heating rate of 5 K min^{-1} and then at 500 °C for 4 h. Xerogel catalysts were prepared by the same procedure used for the preparation of aerogel catalysts except that the drying of xerogel was performed at 120 °C for 12 h.

2.2. Reaction test

Reaction tests were carried out in a continuous flow fixed-bed reactor. The reactor was made of a Pyrex® tube with an i.d. of 0.0254 m. A condenser was attached at the effluent side of the reactor, and its temperature was constantly maintained at 110 °C to condense only solid products (sulfur + ammonium thiosulfate). A line filter was installed after the condenser to trap any solid mist which had not been captured by the condenser. From the condenser up to gas chromatography, all the lines and fittings were heated above 120 °C to prevent condensation of water vapor. The flow rate of gas was controlled by a mass flow controller (Brooks MFC 5850E). Water vapor was introduced to the reactant stream using an evaporator filled with small glass beads, and its amount was controlled by a syringe pump.

The content of effluent gas was analyzed by a gas chromatography (HP 5890) equipped with a thermal conductivity detector and a 1.83 m Porapak T column (80–100 mesh) at 100 °C. The exit gas from the analyzer was passed through a trap containing a concentrated NaOH solution and vented out to a hood. The conversion of H_2S and the selectivity to a special product are defined as follows:

$$\text{conversion of } H_2S\,(X,\%) = \frac{[H_2S]_{\text{inlet}} - [H_2S]_{\text{outlet}}}{[H_2S]_{\text{inlet}}} \times 100$$

$$\text{selectivity } (S,\%) \text{ to a special product } (SO_2, S, \text{ATS}) = \frac{[\text{product}]_{\text{outlet}}}{[H_2S]_{\text{inlet}} - [H_2S]_{\text{outlet}}} \times 100$$

For the calculation of ATS selectivity, moles of ATS was multiplied by a factor of 2 because 1 mol of ATS can be obtained from 2 mol of H_2S.

2.3. Characterization of catalysts

The surface areas and pore size distributions of the catalysts were measured by N_2 adsorption method using the BET technique (Micromeritics ASAP 2000). The phase analysis was performed by X-ray diffraction crystallography with Cu Kα radiation (Rigaku, DMAX 2400). The 2θ range between 5° and 90° was scanned at a rate of 2 °/min. Identification of the phases was carried out by using JCPDS data base. Raman spectroscopy (Bruker IFS66/S, FTIR/Raman) was conducted to investigate the surface structure of catalysts. In order to study the redox characteristics of the catalyst, TPR was carried out. Before reduction, samples were pretreated by heating under air flow from 25 to 450 °C at 10 °C/min. Reduction was achieved under a H_2/N_2 gas mixture (10 vol.% H_2). Gas flow was 20 mL/min and temperature program was from 25 to 800 °C at a heating rate of 10 °C/min and maintained at 800 °C for 1 h.

3. Results and discussion

3.1. Catalyst characterization

V_2O_5–TiO_2 aerogel catalysts with different content of vanadia, 5 wt.% V_2O_5–TiO_2 xerogel, and 5 wt.% impregnated V_2O_5–TiO_2 catalysts were prepared. BET surface areas, pore volume, and average pore diameter are listed in Table 1. Aerogel catalysts showed much higher surface areas and pore volumes than those of xerogel and impregnated V_2O_5–TiO_2. As the contents of vanadia increased, surface area decreased.

Table 1
Specific surface area (S_{BET}), total pore volume (V_p) and average pore size (D_p) of vanadia–titania catalysts

Type	V_2O_5 (wt.%)	S_{BET} (m^2/g)	V_p (cm^3/g)	D_p (nm)
Aerogel	2	160	0.55	13.8
Aerogel	5	153	0.65	14.9
Aerogel	10	127	0.83	25.3
Xerogel	5	13	0.02	6.5
Impregnated	5	55	0.32	23.2

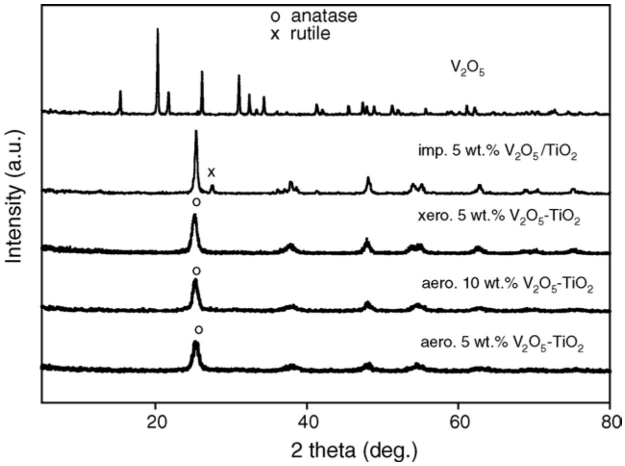

Fig. 1. X-ray diffraction patterns of pure V_2O_5 and V_2O_5–TiO_2 aerogels, xerogel and impregnated V_2O_5–TiO_2 catalysts.

However, pore volume and pore diameter increased. Almost monomodal pore size distribution was observed for the three aerogel catalysts.

Fig. 1 shows the typical XRD peaks attributed to the anatase, rutile, and V_2O_5 of the different types of catalysts and pure V_2O_5. For the aerogel catalysts with 5 and 10 wt.% V_2O_5 and 5 wt.% xerogel catalyst, rutile peak was not observed. But impregnated V_2O_5–TiO_2 catalyst showed a small peak of rutile (1 1 0) face. In a separate experiment, 15 wt.% V_2O_5–TiO_2 aerogel showed quite a big peak of the rutile face. Peaks associated with crystalline V_2O_5 are not observed for any V_2O_5–TiO_2 aerogel catalysts, indicating the effective distribution of vanadium on the titania matrix.

Raman spectra of the catalysts are presented in Fig. 2, and the vibrational modes are summarized in Table 2. The spectra show well-defined adsorption band at 1030 cm^{-1} and a broad band from 900 to 960 cm^{-1}. The band at 1030 cm^{-1} is attributed to monomeric vanadyl species bound directly to the TiO_2 support [18,19]. The broad band in the region from 900 to 960 cm^{-1} and centered at 920 or 930 cm^{-1} is assigned to the terminal and internal V═O stretching vibration, ν(V═O), of polyvanadate groups. The Raman spectra of the 5 wt.% impregnated V_2O_5–TiO_2 exhibit a band at 995 cm^{-1}, characteristics of crystalline V_2O_5 [20]. But, the aerogel catalysts do not show the peaks of crystalline V_2O_5. It means that the aerogel catalysts have uniform distribution of vanadium in the titania matrix.

Table 2
Summary of Raman vibrational frequencies

Type	V_2O_5 (wt.%)	Catalyst		
		Monovanadate (V═O)	Bulk vanadia (V═O)	Polyvanadate (V═O)
Aerogel	2	–	–	930
Aerogel	5	1030	–	930
Aerogel	10	1030	–	930
Impregnated	5	–	995	920

The role of TiO_2 in V_2O_5–TiO_2 catalyst has also been studied by several authors [9,21–23] and is well reviewed by Wachs and Weckhuysen [9]. The terminal V═O bonds have been proposed by many investigators to contain critical oxygen involved in hydrocarbon oxidation reactions over supported vanadia catalysts [24]. However, the combination of in situ Raman and hydrocarbon oxidation reactivity studies [25] have suggested that the terminal V═O bonds and V–O–V bonds do not critically influence the oxidation reactions. The bridging V–O–support bond appears to be the most critical bond which can change the TOF for hydrocarbon oxidation reactions.

TPR with hydrogen is a useful technique to characterize the reduction behavior of the surface active species on a catalyst. The ease of reduction is conveniently measured by the temperature of maximum hydrogen consumption (T_{max}), which increases as the ease of reduction decreases. Fig. 3 shows TPR profiles for the V_2O_5–TiO_2 aerogel catalysts of 2, 5, 10, and 15 wt.% V_2O_5. The TPR profile of the impregnated 5 wt.% V_2O_5–TiO_2 is also reported in Fig. 3. T_{max} of the aerogel

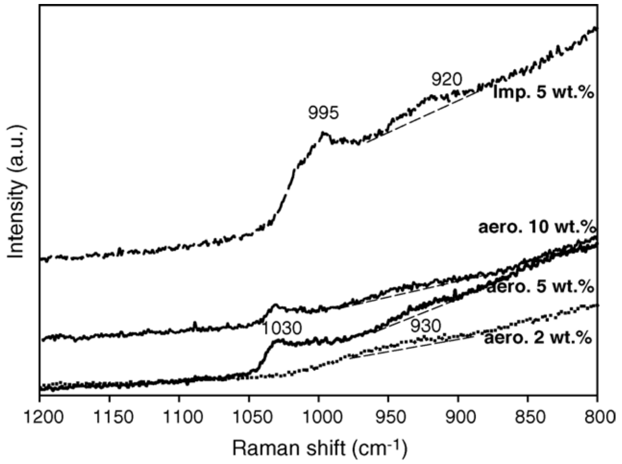

Fig. 2. Raman spectra of V_2O_5–TiO_2 aerogels and impregnated V_2O_5–TiO_2 catalysts.

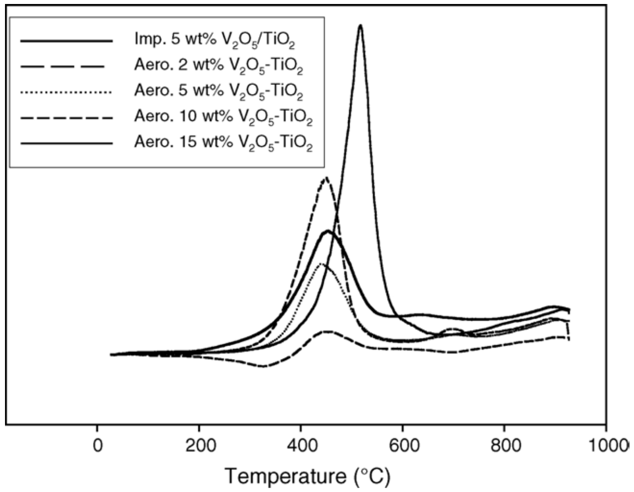

Fig. 3. TPR profiles of V_2O_5–TiO_2 aerogels and impregnated V_2O_5–TiO_2 catalysts.

catalysts of 2, 5, 10, and 15 wt.% V_2O_5 was 440, 442, 451, and 517 °C, respectively. It increased with increasing V_2O_5 wt.%, indicating a decrease in the reducibility of surface. A shift to higher T_{max} with higher V_2O_5 content was also observed for V_2O_5–TiO_2 systems [26,27]. It has been suggested [28], for the vanadium containing oxides, that tetrahedrally co-ordinated V^{5+} species are more difficult to reduce compared with the octahedrally co-ordinated ones, because of the decreased availability of the stronger bonded oxygens. It is generally accepted [29,30] that smaller crystallites are reduced more rapidly than larger crystallites. It can also be observed that the impregnated 5 wt.% V_2O_5–TiO_2 catalyst shows a little higher T_{max} (452 °C) compared to that for 5 wt.% V_2O_5–TiO_2 aerogel catalyst. It means that VO_x are more highly dispersed in the aerogel catalysts (T_{max} = 442 °C), indicating an increase in the reducibility of the surface.

3.2. Selective oxidation of H_2S to S and ATS

Table 3 shows H_2S conversion and selectivity to SO_2 for 5 wt.% V_2O_5–TiO_2 aerogel catalyst with various compositions of reactant mixture at 260 °C. The aerogel catalyst shows high conversion of H_2S without any considerable amount of SO_2 production.

It is known that the following elementary reactions occur in the Claus process, where there is no existence of ammonia [31]:

$$2H_2S + O_2 \rightarrow (2/n)S_n + 2H_2O \tag{1}$$

$$(1/n)S_n + O_2 \rightarrow SO_2 \tag{2}$$

$$2H_2S + 3O_2 \rightarrow 2SO_2 + 2H_2O \tag{3}$$

$$2H_2S + SO_2 \leftrightarrow (3/n)S_n + 2H_2O \tag{4}$$

Ammonia is also known to react easily with H_2S to form ammonium sulfide [$(NH_4)_2S$] which can be oxidized to produce elemental sulfur [32]:

$$H_2S + 2NH_3 \leftrightarrow (NH_4)_2S \tag{5}$$

$$(NH_4)_2S + (1/2)O_2 \rightarrow S + 2NH_3 + H_2O \tag{6}$$

The higher value of H_2S conversion in run B, compared to run A, might be due to the reaction of H_2S and NH_3 (Eq. (5)). In run C, where H_2S was present with excess water and ammonia, the conversion of H_2S was lower than that of run B probably because of inhibition by H_2O (Eq. (4)). However, SO_2 was not produced at all. It is well known [33,34] that NH_3 and SO_2 react to form products such as NH_3SO_2 and $(NH_3)_2SO_2$ under anhydrous conditions. Hartley and Matterson [35] also reported the formation of ammonium bisulfite or ammonium sulfite (Eq. (7)) from the reaction of SO_2 and NH_3 in the presence of water:

$$SO_2 + 2NH_3 + H_2O \rightarrow (NH_4)_2SO_3 \tag{7}$$

From these results, one can conclude that SO_2 formed during the oxidation reaction (Eqs. (2) and (3)) in run C readily reacts with ammonia to form ammonium sulfite or ammonium sulfate. Ammonium thiosulfate (ATS) is commercially produced by the reaction of ammonium sulfite with excess sulfur [36]:

$$(NH_4)_2SO_3 + S \rightarrow (NH_4)_2S_2O_3 \tag{8}$$

Zey et al. [6] reported the following reaction for the production of ATS in the Claus tail gas process, where SO_2 absorption occurs in the ammonia-sulfur dioxide scrubber using aqueous ammonia solution:

$$H_2S + NH_4HSO_3 + (NH_4)_2SO_3 \rightarrow (3/2)(NH_4)_2S_2O_3 + (3/2)H_2O \tag{9}$$

Therefore, it is believed that SO_2 may be consumed to form ammonium thiosulfate.

Table 4 lists H_2S conversions of V_2O_5–TiO_2 aerogels, xerogel, and impregnated catalysts at reaction temperatures of 220–300 °C after 2 h of reaction at each temperature. All the aerogel catalysts showed nearly 100% of H_2S conversion without any considerable emission of sulfur dioxide, which is known to be produced by either deep oxidation of sulfur or H_2S, or by the reverse Claus reaction (Eq. (4)). The produced SO_2 may be considered to react with ammonia to produce ATS via ammonium sulfite (Eq. (7)). However, xerogel and impregnated catalysts showed much lower H_2S conversion than the aerogel catalysts. The high catalytic activity of the aerogel catalysts may be due to their high surface area and highly homogeneous VO_x dispersion on the surface.

The effects of temperature on the product selectivities were studied with 5 wt.% V_2O_5–TiO_2 aerogel catalyst, and the selectivities to S and ATS, and H_2S conversions are listed in

Table 3
H_2S conversion and selectivity to SO_2 with various compositions of reactant mixture at 260 °C

Run	Reactant composition (vol.%)				X-H_2S (%)	S-SO_2 (%)
	H_2S	O_2	NH_3	H_2O		
A	5	2.5	–	–	97.0	3.8
B	5	2.5	5	–	100	0
C	5	2.5	5	60	99.1	0

Reaction condition: GHSV = 30,000 h^{-1}, reaction time = 6 h.

Table 4
Conversion of H_2S for vanadia–titania of catalysts at different temperatures

Catalysts	V_2O_5 (wt.%)	H_2S conversion (%)				
		220 °C	240 °C	260 °C	280 °C	300 °C
Aerogel	2	100	100	100	100	100
Aerogel	5	100	100	100	100	100
Aerogel	10	95.2	97.4	100	100	100
Xerogel	5	46.5	57.6	79.3	84.2	90.0
Impregnated	5	78.6	78.8	80.8	76.5	70.1

Reaction condition: $H_2S/O_2/NH_3/H_2O/He$ = 5/2.5/5/60/27.5, GHSV = 30,000 h^{-1}, reaction time = 2 h.

Table 5
Conversion of H_2S and selectivities to products for 5 wt.% V_2O_5–TiO_2 catalysts at different reaction temperatures

	Temperature (°C)	X-H_2S (%)	S-SO_2 (%)	S-S (%)	S-ATS (%)
Aerogel	220	93.8	0	45.2	54.8
Aerogel	240	96.9	0	42.1	57.9
Aerogel	260	99.1	0	39.3	60.7
Aerogel	280	98.6	0	33.1	66.9
Aerogel	300	98.0	0	25.5	74.5
Xerogel	260	78.1	8.8	35.8	55.4
Impregnated	260	79.7	0	61.4	38.6

Reaction condition: $H_2S/O_2/NH_3/H_2O/He = 5/2.5/5/60/27.5$, GHSV = 30,000 h^{-1}, reaction time = 6 h.

Table 5. The conversion of H_2S were measured after 6 h of reaction, since the initial conversion of H_2S decreased up to about 5 h and it maintained constant during 3 days of reaction test. The catalyst showed maximum H_2S conversion at 260 °C, then the activity decreased slightly with increasing temperature. Table 5 also shows that the S-ATS increased but S-S decreased with increasing temperature. As reported in other previous works [37,38], higher temperature yielded more production of SO_2 and less production of elemental sulfur than low temperature did in the H_2S oxidation without NH_3. With the presence of NH_3, the produced SO_2 can react to form $(NH_4)_2SO_3$, then finally to produce ATS by the reactions of Eqs. (7) and (8). Five weight percent xerogel and impregnated catalysts showed much lower H_2S conversions than the aerogel catalyst. Xerogel showed the production of SO_2 with the selectivity of 8.8%.

4. Conclusions

The selective oxidation of hydrogen sulfide in the presence of excess water and ammonia was investigated in this study. V_2O_5–TiO_2 aerogel catalysts showed very high conversion of H_2S without any considerable amount of SO_2 emission. These catalysts showed much higher surface area and better dispersion of VO_x on the surface compared to xerogel and impregnated catalysts. For the aerogel catalysts, two species of surface vanadium have been identified by Raman spectroscopy: monomeric vanadyl and polymeric vanadates. The impregnated V_2O_5–TiO_2 catalyst did not have monovanadate peak, but it showed a bulk vanadia peak. Temperature programmed reduction (TPR), XRD and Raman analyses revealed that the high catalytic performance of the aerogel catalysts originated from their high surface area, good VO_x dispersion, and high reducibility.

Acknowledgements

This work was supported by the Korea Research Foundation Grant (KRF-2005-100826), and the Brain Korea 21 and Brain Busan 21 programs.

References

[1] B.G. Goar, Oil Gas J. 25 (1975) 96.
[2] R. Lell, Sulphur 178 (1985) 29.
[3] B.G. Kim, D.W. Park, I. Kim, H.C. Woo, Catal. Today 87 (2003) 11.
[4] D.W. Park, B.K. Park, D.K. Park, H.C. Woo, Appl. Catal. A: Gen. 223 (2002) 215.
[5] D.W. Park, B.G. Kim, M.I. Kim, I. Kim, H.C. Woo, Catal. Today 93 (2004) 235.
[6] A. Zey, S. White, D. Johnson, Chem. Eng. Prog. 76 (10) (1980) 76.
[7] J.F. Benito, E.S. Patent 547 (1986) 563.
[8] G. Centi, Appl. Catal. A 147 (1996) 267.
[9] I.E. Wachs, B.T. Weckhuysen, Appl. Catal. A 157 (1997) 67.
[10] G.M. Pajonk, Appl. Catal. 72 (1991) 217.
[11] M.A. Cauqui, J.M. Rodriquez-Iziquierdo, J. Non-Cryst. Solids 147/148 (1992) 724.
[12] M. Schneider, M. Maciejewski, S. Tschudin, A. Wokaun, A. Baiker, J. Catal. 149 (1994) 326.
[13] J.B. Miller, S.T. Johnston, E.I. Ko, J. Catal. 150 (1994) 311.
[14] C. Hoang-Van, O. Zegaoui, P. Richat, J. Non-Cryst. Solids 225 (1998) 157.
[15] O. Zegaoui, C. Hoang-Van, M. Karroura, Appl. Catal. B 9 (1996) 211.
[16] M.A. Reiche, E. Ortelli, A. Baiker, Appl. Catal. B 23 (1999) 187.
[17] G. Centi, D. Pinelli, F. Trifiro, D. Ghoussoub, M. Guelton, L. Gengembre, J. Catal. 130 (1991) 238.
[18] G.T. Went, L.-J. Leu, A.T. Bell, J. Catal. 134 (1992) 492.
[19] F. Prinetto, G. Ghiotti, M. Occhiuzzi, V. Indovina, J. Phys. Chem. B 102 (1998) 10316.
[20] S.S. Chan, I.E. Wachs, L.L. Murrell, L. Wang, W. Keith Hall, J. Phys. Chem. 88 (1984) 5381.
[21] H. Bosh, F.J. Janssen, Catal. Today 2 (1988) 369.
[22] G. Centi, Appl. Catal. A 147 (1996) 267.
[23] C. Doornkamp, M. Clement, X. Gao, I.E. Wachs, V. Ponec, J. Catal. 185 (1999) 415.
[24] G.C. Bond, J.C. Vedrine, Catal. Today 20 (1994) 1.
[25] N. Arora, G. Deo, I.E. Wachs, A.M. Hirt, J. Catal. 159 (1996) 1.
[26] A. Baiker, P. Dollenmeier, M. Glinski, A. Reller, Appl. Catal. 35 (1987) 351.
[27] R.A. Koepple, J. Nickl, A. Baiker, Catal. Today 20 (1994) 45.
[28] G. Lischke, W. Hanke, H.G. Jerschkewitz, G. Ohlmann, J. Catal. 91 (1985) 54.
[29] G. Bond, J. Perez Zurita, S. Flaerz, P.J. Gellings, H. Bosch, J.G. VanHommen, B.J. Kip, Appl. Catal. 22 (1986) 361.
[30] D. Patel, P.J. Andersen, H.H. Kung, J. Catal. 125 (1990) 132.
[31] R.J.A.M. Terorde, P.J. van den Brink, L.M. Visser, A.J. van Dillen, J.W. Geus, Catal. Today 17 (1993) 217.
[32] D. Chang, M.C. McGaugh, US Patent No. 4,765,969 (1988).
[33] R. Landreth, R.G. de Penta, J. Heicklen, J. Phys. Chem. 89 (1985) 1690.
[34] W.D. Scott, D. Lamb, J. Am. Chem. Soc. 92 (1970) 3943.
[35] E.M. Hartley, M.J. Matterson, Ind. Eng. Chem. Fundam. 14 (1975) 67.
[36] K.H. Henke, G. Weiner, Ger. Offen. No. 2,635,649 (1978).
[37] S.W. Chun, J.Y. Jang, D.W. Park, H.C. Woo, J.S. Chung, Appl. Catal. B 16 (1998) 235.
[38] M.Y. Shin, D.W. Park, J.S. Chung, Appl. Catal. B 30 (2001) 409.